Computational and Applied Mathematics (2024) 43:395
https://doi.org/10.1007/s40314-024-02902-4

Higher-order methods for the Poisson equation obtained with geometric multigrid and completed Richardson extrapolation

Luciano Pereira da Silva[1] · Marcio Augusto Villela Pinto[2] · Luciano Kiyoshi Araki[2]

Received: 10 January 2024 / Revised: 15 July 2024 / Accepted: 12 August 2024

Abstract
The study presented in this paper consists of a grouping of methods for determining numerical solutions to the Poisson equation (heat diffusion) with high accuracy. We compare the results obtained with classical second-order finite difference method (CDS-2) with fourth-order compact (CCDS-4) and the exponential methods (EXP-4). We accelerate the convergence of the numerical solutions using the geometric multigrid method and then apply the completed Richardson extrapolation (CRE) across the full temperature field. This proposed clustering determined solutions with two orders of accuracy higher for all three methods presented in the study, in addition to recommending the EXP-4 method together with CRE for its accuracy and low computational effort. The evidence for our results was established through qualitative verification, through the assessment of orders of accuracy of the discretization error; and quantitative verification, through the analysis of CPU time and complexity order of the numerical solutions calculated. The numerical solutions of sixth-order of accuracy obtained after proposed CRE methodology using the CCDS-4 and EXP-4 methods are recognized as benchmark solutions for these two classes of methods.

Keywords Higher-order methods · Geometric multigrid · Heat diffusion · Discretization error · Verification

Mathematics Subject Classification 65N06 · 65N55 · 65M06 · 65L20 · 74S30

Marcio Augusto Villela Pinto and Luciano Kiyoshi Araki have contributed equally to this work.

✉ Luciano Pereira da Silva
luciano.silva@ufpr.br; lucianocogo@gmail.com

Marcio Augusto Villela Pinto
marcio_villela@ufpr.br

Luciano Kiyoshi Araki
lucaraki@ufpr.br

[1] Laboratory of Numerical Experimentation (LENA), Department of Mechanical Engineering (DEMEC), Federal University of Parana (UFPR), Francisco Heraclito dos Santos, P.O. Box 19040, Curitiba Zip Code 81531-980, Parana, Brazil

[2] Department of Mechanical Engineering (DEMEC), Federal University of Parana (UFPR), Francisco Heraclito dos Santos, P.O. Box 19040, Curitiba Zip Code 81531-980, Parana, Brazil

Published online: 05 September 2024

1 Introduction

One of the greatest challenges of Computational Fluid Dynamics (CFD) is to obtain improved methods related to the good level of accuracy of the numerical solutions. In particular, one of these challenges is characterized by the determination of the numerical solution of the continuity equation, which can be represented by a Poisson equation under certain circumstances: steady-state, and velocities modeled by a potential equation, which requires a large computational effort. The Poisson equation is given by

$$\frac{\partial^2 \boldsymbol{\Psi}}{\partial x^2} + \frac{\partial^2 \boldsymbol{\Psi}}{\partial y^2} = -f(x, y) \ \ in \ \ \Omega, \tag{1}$$

with Dirichlet boundary conditions that agree with the analytical solution. In this equation, $\boldsymbol{\Psi} \in C^{\infty}(\Omega)$ is the diffusion property, in our case, the temperature; x and y are the coordinate directions and f is the source term.

Poisson equation is also well known for modeling the actual physical phenomenon of steady-state heat diffusion.

Among all sources of numerical error, the discretization error is usually the most significant one (Marchi and da Silva 2002). In general, the decrease in the discretization error is associated with highly refined grids which require very high computational effort to achieve a numerical solution. To determine such solutions with higher-order of accuracy, the post-processing method known as Repeated Richardson Extrapolation (RRE) can be used (Marchi et al. 2013a, b; Cheney and Kincaid 2012). In order to reduce the discretization error, estimators were proposed in Marchi et al. (2013a), Marchi et al. (2016) that presented and tested a numerical procedure using RRE applied to problems such as those described by Poisson 1D, Laplace 2D, Burgers 2D, and incompressible Navier-Stokes 2D equations. Although all cited works (Marchi et al. 2013a, b; Cheney and Kincaid 2012) obtained reduced discretization errors, none of them neither used multigrid methods nor obtained more accurate results for the full domain.

Some studies present higher-order methods for discretizing Eq. (1) based on Finite Difference Method (FDM) (Burden et al. 2016). These methods are: the Compact Finite Difference Scheme of fourth-order (CCDS-4) (Wang and Zhang 2009); and an unconventional compact nine points, named as Exponential Finite Difference Scheme (EXP-4) (Pandey 2013; da Silva et al. 2021). In addition, the higher-order methods in conjunction with the standard multigrid Full Approximation Scheme (FAS) (Trottenberg et al. 2000) provide faster convergence to the numerical solution.

In Wang and Zhang (2009), the authors designed a new sixth-order compact scheme with a multigrid method (MG) and Richardson extrapolation (RE) to solve the 2D Poisson equation. This method is based on designing a MG to compute the approximate solution using the fourth-order compact scheme in both the fine and the coarse grids. Also, the authors proposed with a new iterative interpolation scheme combined with the RE to achieve sixth-order accuracy on the fine grid. The proposed scheme of Wang and Zhang (2009) modified the MG method, changing the restriction and prolongation operators. The goal of the current work, however, is proposing the use of RE as a post-processing methodology, not modifying the MG method.

In Koroche and Chemeda (2021), a sixth-order compact FDM was presented to solve the 1D KdV-Burger equation. The authors concluded that the results obtained were more convenient, reliable, and effective than some methods of the listed in the literature by decreasing the value of h and Δt. Chemeda and Merga (2021) presented a fourth-order compact FDM combined with RE for solving the 1D heat diffusion equation. Two model problems were con-

sidered and solved for different values of the spatial and temporal step lengths. The proposed method is unconditionally stable, consistent and generates accurate numerical solutions. In Chemeda et al. (2022), the authors presented a the fourth-order compact Crank-Nicolson scheme combined with RE for solving the 1D Fisher's equation. The space derivative was discretized by the fourth-order compact FDM, the nonlinear term was linearized by the lagging method, and the temporal derivative was discretized by the modified Crank-Nicolson scheme. The authors concluded that the order of the method improved from fourth- to sixth-order in the space direction. However, none of the cited works employed neither complete Richardson extrapolation (CRE) nor multigrid to achieve their results.

In da Silva et al. (2021), the authors showed how to improve the order for accuracy of the 2D Poisson equation by combining the RRE method with high-order schemes to find solutions of sixth-, eighth-, and tenth-order of accuracy. The authors also compared compact and exponential finite difference schemes of fourth-order. The contribution is also based on a process that initializes with fourth-order solutions and the multigrid Full Approximation Scheme (FAS) applied to accelerate the convergence on the fine grids.

Dai et al. (2017) presented a high-accuracy and efficient method for solving anisotropic Poisson equations. The completed Richardson extrapolation (CRE) was applied to compute sixth-order solutions through two fourth-order solutions from different scale grids. The partial semi-coarsening MG was employed to solve the resulting linear systems. Multiscale MG was involved in accelerating the computation procedure. Different computational techniques were discussed for 2D and 3D cases. Hu et al. (2022) presented an accelerated multiscale Newton-multigrid method to solve a 2D Poisson equation with a nonlinear forcing term, based on fourth-order compact difference schemes and extrapolation strategies. In that new approach, the extrapolation effectively reduces the number of iterations and the total computational cost. In addition, a CRE strategy is introduced to generate extrapolated solutions with higher-order of accuracy than the method used to discretize the equation, and at low cost.

In da Silva et al. (2020), the authors presented a completed repeated Richardson extrapolation (CRRE) procedure for a more generic type of grid not necessarily with coincident nodes, and tested it on compressible fluid flows. The procedure proposed can increase the achieved accuracy and significantly decrease the magnitude of the spatial error in all problems tested. It must be observed, however, that all studied equations represented one- or quasi-one dimensional problems, subjected to discontinuities of variables of interest.

Summarizing, there are several authors who studied forth- or higher-order of accuracy to solve with multigrid two-dimensional problems, such as Wang and Zhang (2009), Dai et al. (2017), Hu et al. (2022), Gordin and Shadrin (2023), Hu et al. (2023). Although all of them obtained high accurate numerical solutions for their problems, the focus of such works were improving interpolation schemes used in discretization. Some of them used RE in order to improve the solution accuracy. However, none of them employed CRE to achieve high order of accuracy to the full domain.

The main goal of this work is to obtain sixth-order of accuracy solutions for Eq. (1) in an efficient way without increasing the computational time compared to the classical fourth-order methods studied here. For this, we start the procedure with fourth-order solutions given by Exponential Finite Difference Scheme. Then, we achieve sixth-order of accuracy using the CRE. For the calculations, we accelerate them with the MG on the fine grids and we use quadruple precision (Real*16 or extended precision) with the FORTRAN language.

This work is divided as follows: in Sect. 2, we present the mathematical and numerical models; in Sect. 3, the higher-order methods; in Sect. 4, the methodology used in our study; in Sect. 5, the numerical results; and in Sect. 6, concluding remarks.

2 Mathematical and numerical models

In this section we cover the mathematical and numerical models already shown in da Silva et al. (2020). We have chosen to present these models to facilitate the development of the study and allow its exploration. The details of such models are not exhaustive and allow a better understanding of our proposal when applying the post-processing technique in this study to increase the order of accuracy and, consequently, reduce the discretization error.

Remark 1 As the CRE is a post-processing (da Silva et al. 2020), this technique can be generalized, as it uses assumptions that are easily fulfilled (monotonic convergence), and for any type of grid (in unstructured grids we can use AMG). On the other hand, in cases where there is no monotonicity, we can use interpolation and optimization techniques, such as those used in Marchi et al. (2016).

Thus, as in da Silva et al. (2020), the computational domain remains the unit square $\Omega = [0, 1] \times [0, 1]$, with boundary conditions described by the analytical solution, and the meshes used are uniform. The mesh elements h and k are described by $h = 1/(N_x - 1)$ and $k = 1/(N_y - 1)$, where $N_x = N_y = \{9, 17, 33, \ldots, 2049, 4097\}$ are number points of meshes in $x-$ and $y-$direction, respectively.

Revisiting the called Central Difference Scheme of second-order (CDS-2), presented in da Silva et al. (2020), we have

$$\frac{\partial^2 \boldsymbol{\Psi}}{\partial x^2}|_{i,j} = \frac{\boldsymbol{\Psi}_{i-1,j} - 2\boldsymbol{\Psi}_{i,j} + \boldsymbol{\Psi}_{i+1,j}}{h^2} - \frac{h^2}{12}\frac{\partial^4 \boldsymbol{\Psi}}{\partial x^4}|_{i,j} - \frac{h^4}{360}\frac{\partial^6 \boldsymbol{\Psi}}{\partial x^6}|_{i,j} + O(h^6) \quad (2)$$

to approximate the derivative in the $x-$direction and,

$$\frac{\partial^2 \boldsymbol{\Psi}}{\partial y^2}|_{i,j} = \frac{\boldsymbol{\Psi}_{i,j-1} - 2\boldsymbol{\Psi}_{i,j} + \boldsymbol{\Psi}_{i,j+1}}{k^2} - \frac{k^2}{12}\frac{\partial^4 \boldsymbol{\Psi}}{\partial y^4}|_{i,j} - \frac{k^4}{360}\frac{\partial^6 \boldsymbol{\Psi}}{\partial y^6}|_{i,j} + O(k^6), \quad (3)$$

for $y-$direction. Here, we use the spatial notation (i, j) to denote the center point of the discretization; $i-1, i+1$ their spatial $x-$neighbors; and $j-1, j+1$ their spatial $y-$neighbors.

By substituting Eqs. (2) and (3) in Eq. (1) and after some mathematical manipulations, we determine the CDS-2 approximation, as shown in

$$\frac{\boldsymbol{\psi}_{i-1,j} - 2\boldsymbol{\psi}_{i,j} + \boldsymbol{\psi}_{i+1,j}}{h^2} + \frac{\boldsymbol{\psi}_{i,j-1} - 2\boldsymbol{\psi}_{i,j} + \boldsymbol{\psi}_{i,j+1}}{k^2} = -f_{i,j}. \quad (4)$$

Notice that the analytical solution, $\boldsymbol{\Psi}$, has been replaced by the numerical solution, $\boldsymbol{\psi}$. This was done because the analytical solution is unknown. The approximations of Eqs. (2) and (3) generate the a priori asymptotic order $p_0 = 2$ and true a priori orders of discretization error $p_m = 2, 4, 6, \ldots$ in Eq. (4) (Marchi and da Silva 2002). In the next section we describe how to increase the order of this discretization method to two well-known higher-order methods. Below we give the representation of the analytic expression of the local truncation error considering $k = h$

$$\varepsilon_\tau(\boldsymbol{\Psi}) = -\frac{h^2}{12}\left(\frac{\partial^4 \boldsymbol{\Psi}}{\partial x^4} + \frac{\partial^4 \boldsymbol{\Psi}}{\partial y^4}\right) - \frac{h^4}{360}\left(\frac{\partial^6 \boldsymbol{\Psi}}{\partial x^6} + \frac{\partial^6 \boldsymbol{\Psi}}{\partial y^6}\right) + O(h^6). \quad (5)$$

3 Higher-order methods for the Poisson equation

In this section we present the compact and exponential finite difference schemes, which are the higher-order methods used in this work.

3.1 Compact finite difference scheme

Considering the problem given by Eq. (1) and its second-order numerical solution $\boldsymbol{\psi}$ given by Eq. (4), we determine approximations for the fourth-order derivatives in order to obtain the well-known Compact Finite Difference Scheme of fourth-order (CCDS-4). For this, we expand the following terms:

$$\frac{\partial^4 \boldsymbol{\Psi}}{\partial x^4}|_{i,j} = -\frac{\partial^2 f}{\partial x^2}|_{i,j} - \frac{\partial^4 \boldsymbol{\Psi}}{\partial x^2 \partial y^2}|_{i,j} \tag{6}$$

to approximate the derivative in the $x-$direction and,

$$\frac{\partial^4 \boldsymbol{\Psi}}{\partial y^4}|_{i,j} = -\frac{\partial^2 f}{\partial y^2}|_{i,j} - \frac{\partial^4 \boldsymbol{\Psi}}{\partial x^2 \partial y^2}|_{i,j}, \tag{7}$$

to approximate the derivative in the $y-$direction.

Now we substitute the Eqs. (6) and (7) in Eqs. (2) and (3), respectively, and approximating the partial second-order derivative using CDS-2, we determine

$$\begin{aligned}\frac{\partial^2 \boldsymbol{\Psi}}{\partial x^2}|_{i,j} = &\frac{\boldsymbol{\Psi}_{i-1,j} - 2\boldsymbol{\Psi}_{i,j} + \boldsymbol{\Psi}_{i+1,j}}{h^2} + \frac{1}{12}(f_{i-1,j} - 2f_{i,j} + f_{i+1,j}) \\ &+ \frac{h^2}{12}\frac{\partial^4 \boldsymbol{\Psi}}{\partial x^2 \partial y^2}|_{i,j} - \frac{h^4}{144}\frac{\partial^4 \boldsymbol{\Psi}}{\partial x^4}|_{i,j} + O(h^4)\end{aligned} \tag{8}$$

to approximate the derivative in the x-direction and,

$$\begin{aligned}\frac{\partial^2 \boldsymbol{\Psi}}{\partial y^2}|_{i,j} = &\frac{\boldsymbol{\Psi}_{i,j-1} - 2\boldsymbol{\Psi}_{i,j} + \boldsymbol{\Psi}_{i,j+1}}{k^2} + \frac{1}{12}(f_{i,j-1} - 2f_{i,j} + f_{i,j+1}) \\ &+ \frac{k^2}{12}\frac{\partial^4 \boldsymbol{\Psi}}{\partial x^2 \partial y^2}|_{i,j} - \frac{k^4}{144}\frac{\partial^4 \boldsymbol{\Psi}}{\partial y^4}|_{i,j} + O(k^4).\end{aligned} \tag{9}$$

to $y-$direction.

For the fourth-order derivative $\partial^4 \boldsymbol{\Psi}/(\partial x^2 \partial y^2)|_{i,j}$, we obtain the following approximations

$$\begin{aligned}\frac{\partial^4 \boldsymbol{\Psi}}{\partial x^2 \partial y^2}|_{i,j} = &\frac{4\boldsymbol{\Psi}_{i,j}}{h^2 k^2} - 2\left(\frac{\boldsymbol{\Psi}_{i-1,j} + \boldsymbol{\Psi}_{i+1,j} + \boldsymbol{\Psi}_{i,j-1} + \boldsymbol{\Psi}_{i,j-1}}{h^2 k^2}\right) \\ &+ \frac{\boldsymbol{\Psi}_{i-1,j-1} + \boldsymbol{\Psi}_{i-1,j+1} + \boldsymbol{\Psi}_{i+1,j-1} + \boldsymbol{\Psi}_{i+1,j+1}}{h^2 k^2} + O(h^2, k^2).\end{aligned} \tag{10}$$

Now, we substitute the approximations given in Eq. (10) into their respective derivatives contained in Eqs. (8) and (9). After some mathematical manipulations, we determined the following approximations

$$\frac{\boldsymbol{\psi}_{i-1,j}-2\boldsymbol{\psi}_{i,j}+\boldsymbol{\psi}_{i+1,j}}{h^2}+\frac{\boldsymbol{\psi}_{i,j-1}-2\boldsymbol{\psi}_{i,j}+\boldsymbol{\psi}_{i,j+1}}{k^2}$$
$$+\left(\frac{h^2+k^2}{12}\right)\left[\frac{4\boldsymbol{\psi}_{i,j}}{h^2k^2}-2\left(\frac{\boldsymbol{\psi}_{i-1,j}+\boldsymbol{\psi}_{i+1,j}+\boldsymbol{\psi}_{i,j-1}+\boldsymbol{\psi}_{i,j+1}}{h^2k^2}\right)\right.$$
$$\left.+\frac{\boldsymbol{\psi}_{i-1,j-1}+\boldsymbol{\psi}_{i-1,j+1}+\boldsymbol{\psi}_{i+1,j-1}+\boldsymbol{\psi}_{i+1,j+1}}{h^2k^2}\right]$$
$$=\frac{1}{12}(f_{i-1,j}+f_{i+1,j}-8f_{i,j}+f_{i,j-1}+f_{i,j+1}). \tag{11}$$

As we are performing a uniform mesh discretization, then we can make the simplification $k=h$ and rewriting Eq. (11), we get

$$\boldsymbol{\psi}_{i,j}=\frac{3}{10}\left[F_{i,j}+\frac{2}{3}\left(\boldsymbol{\psi}_{i+1,j}+\boldsymbol{\psi}_{i-1,j}+\boldsymbol{\psi}_{i,j-1}+\boldsymbol{\psi}_{i,j+1}\right)\right.$$
$$\left.+\frac{1}{6}\left(\boldsymbol{\psi}_{i+1,j+1}+\boldsymbol{\psi}_{i-1,j+1}+\boldsymbol{\psi}_{i+1,j-1}+\boldsymbol{\psi}_{i-1,j-1}\right)\right]h^2, \tag{12}$$

where F term is

$$F_{i,j}:=\frac{1}{12}(f_{i-1,j}+f_{i+1,j}-8f_{i,j}+f_{i,j-1}+f_{i,j+1}). \tag{13}$$

Again, we replace $\boldsymbol{\Psi}$ by $\boldsymbol{\psi}$ by the same exposed reason, the Eq. (14) does not change because the local truncation error is described in terms of the analytical solution.

In this scheme, the local truncation error is given by Le Veque (2007), as follows

$$\varepsilon_\tau(\boldsymbol{\Psi})=-\frac{h^4}{360}\left(\frac{\partial^6\boldsymbol{\Psi}}{\partial x^6}+\frac{\partial^6\boldsymbol{\Psi}}{\partial y^6}\right)+O(h^6). \tag{14}$$

With this, the Eq. (14) show us the *a priori* asymptotic order is $p_0=4$, and *a priori* true orders, $p_m=4,6,8,\ldots$, for CCDS-4.

By rearranging Eqs. (12) and (13), we can rewrite them to generate the CCDS-4 stencil, which is given by da Silva et al. (2020)

$$\frac{10}{3h^2}\begin{bmatrix}0&0&0\\0&1&0\\0&0&0\end{bmatrix}_h-\frac{2}{3h^2}\begin{bmatrix}0&1&0\\1&0&1\\0&1&0\end{bmatrix}_h-\frac{1}{6h^2}\begin{bmatrix}1&0&1\\0&0&0\\1&0&1\end{bmatrix}_h=\frac{1}{12}\begin{bmatrix}0&1&0\\1&-8&1\\0&1&0\end{bmatrix}_h. \tag{15}$$

The stencil shown from Eq. (15) is based on the approximations of Wang and Zhang (2009), Gupta et al. (1997), Li and Chen (2008) and considers a unit square domain and, uniform grid elements.

3.2 Exponential finite difference scheme

The Exponential Finite Difference Scheme of fourth-order (EXP-4) shown in Pandey (2013), da Silva et al. (2020), Pandey and Pandey (2016), Pandey (2016) is described in the following:

$$\frac{\partial^2\boldsymbol{\Psi}}{\partial x^2}+\frac{\partial^2\boldsymbol{\Psi}}{\partial y^2}=f(x,y)e^{\phi(h)}. \tag{16}$$

As we are performing a uniform mesh discretization, then we can make the simplification $k=h$, replacing the approximations from Eq. (11) on the left hand side of Eq. (16) and,

rewriting it, we get

$$a_o\left(\frac{\boldsymbol{\psi}_{i-1,j}+\boldsymbol{\psi}_{i+1,j}+\boldsymbol{\psi}_{i,j-1}+\boldsymbol{\psi}_{i,j+1}}{h^2}\right) + a_1\left(\frac{\boldsymbol{\psi}_{i-1,j-1}+\boldsymbol{\psi}_{i-1,j+1}+\boldsymbol{\psi}_{i+1,j-1}+\boldsymbol{\psi}_{i+1,j+1}}{h^2}\right)+a_2\boldsymbol{\psi}_{i,j} = b_0 f_{i,j}e^{\phi(h)}, \tag{17}$$

where the variable ϕ is described by

$$\phi(h) = \frac{h^2\nabla^2 f_{i,j}}{12 f_{i,j}}. \tag{18}$$

Note that the laplacian of Eq. (18) has yet to be approximated. In this case, we use the CDS-2, which results in

$$h^2\nabla^2 f_{i,j} = f_{i-1,j}+f_{i+1,j}-4f_{i,j}+f_{i,j-1}+f_{i,j+1}, \tag{19}$$

besides that,

$$\phi(h) = \frac{f_{i-1,j}+f_{i+1,j}-4f_{i,j}+f_{i,j-1}+f_{i,j+1}}{12 f_{i,j}}. \tag{20}$$

We use the constants $a_0 = 4$, $a_1 = 1$, $a_2 = -20$ and, $b_0 = 6$ given in Pandey (2013), da Silva et al. (2020). In this way, we can rewrite Eq. (17) as

$$4\left(\frac{\boldsymbol{\psi}_{i-1,j}+\boldsymbol{\psi}_{i+1,j}-4\boldsymbol{\psi}_{i,j}+\boldsymbol{\psi}_{i,j-1}+\boldsymbol{\psi}_{i,j+1}}{h^2}\right) + \left(\frac{\boldsymbol{\psi}_{i-1,j-1}+\boldsymbol{\psi}_{i-1,j+1}+\boldsymbol{\psi}_{i+1,j-1}+\boldsymbol{\psi}_{i+1,j+1}}{h^2}\right)-20\boldsymbol{\psi}_{i,j} = 6 f_{i,j}e^{\phi(h)}, \tag{21}$$

with local truncation error (Pandey 2013)

$$\varepsilon_\tau(\boldsymbol{\Psi}) = \frac{h^4}{240}\left[4\left(\frac{\partial^6\boldsymbol{\Psi}}{\partial x^6}+5\frac{\partial^6\boldsymbol{\Psi}}{\partial x^4 y^2}+5\frac{\partial^6\boldsymbol{\Psi}}{\partial x^2 y^4}+\frac{\partial^6\boldsymbol{\Psi}}{\partial y^6}\right) - 5\left(\frac{\partial^2\boldsymbol{\Psi}}{\partial x^2}+\frac{\partial^2\boldsymbol{\Psi}}{\partial y^2}\right)^{-1}\left(\frac{\partial^4\boldsymbol{\Psi}}{\partial x^4}+2\frac{\partial^4\boldsymbol{\Psi}}{\partial x^2 y^2}+\frac{\partial^4\boldsymbol{\Psi}}{\partial y^4}\right)^2\right]+O(h^6). \tag{22}$$

Equation (22) determines *a priori* asymptotic order, $p_0 = 4$ and *a priori* true orders, $p_m = 4, 6, 8, \ldots$. of Eq. (21).

By rearranging Eq. (21), we can rewrite them to generate the EXP-4 stencil, which is given by da Silva et al. (2020)

$$\frac{20}{h^2}\begin{bmatrix}0&0&0\\0&1&0\\0&0&0\end{bmatrix}_h - \frac{4}{h^2}\begin{bmatrix}0&1&0\\1&0&1\\0&1&0\end{bmatrix}_h - \frac{1}{h^2}\begin{bmatrix}1&0&1\\0&0&0\\1&0&1\end{bmatrix}_h = -6e^{\phi(h)}\begin{bmatrix}0&0&0\\0&1&0\\0&0&0\end{bmatrix}_h, \tag{23}$$

where the exponential term is given by

$$e^{\phi(h)} = exp\left(\frac{1}{12}\begin{bmatrix}0 & 1 & 0\\ 1 & -4 & 1\\ 0 & 1 & 0\end{bmatrix}_h \Big/ \begin{bmatrix}0 & 0 & 0\\ 0 & 1 & 0\\ 0 & 0 & 0\end{bmatrix}_h\right). \tag{24}$$

The stencils shown from Eqs. (23) and (24) are based on the approximations of Pandey (2013) considering a unit square domain and uniform grid elements.

The stencils of both fourth-order accuracy methods produce sparse and large systems of linear equations with nine diagonals. The solutions of these systems are determined using the lexicographic Gauss-Seidel smoother (Burden et al. 2016) and have convergence acceleration obtained with the geometric multigrid method.

4 Methodology

In this section we present the methodology used in our study. To do this, we will present the basic concepts about the multigrid method, order of accuracy and complexity, in addition to explaining an efficient way to use Richardson extrapolation.

4.1 Multigrid method

We know that the more the grid is refined, the smaller the discretization error. However, highly refined grids result in large-scale systems of linear equations, thus requiring a large computational effort to obtain their numerical solution. So, we will decrease the computational time used with such highly refined grids by adopting the multigrid method (MG) (Trottenberg et al. 2000; Wesseling 2004; Oliveira et al. 2018), which is a method that accelerates the convergence of standard methods using a hierarchy of grids. This method is a powerful numerical tool to determine the solutions addressed in our study.

Classic iterative methods quickly reduce the oscillatory error modes of the finest grid in the initial iterations, but leaving the smooth modes, which makes the method lose its effectiveness (Trottenberg et al. 2000; Pinto et al. 2016; da Silva et al. 2021; Malacarne et al. 2022). With that, we transfer information (residue and/or solution) to the coarser grids (using restriction operators), where the smooth modes become more oscillatory and the method is known to be effective (Trottenberg et al. 2000; Wesseling 2004). When reaching the coarsest possible or desired grid, information (correction) must be returned to the original finer grid of the problem (using prolongation operators). This accelerates the convergence of the method (Pinto et al. 2016; Trottenberg et al. 2000; Wesseling 2004; Oliveira et al. 2018; Santiago et al. 2023; da Silva et al. 2024) because it becomes efficient for all error components (oscillatory and smooth).

The information transferred among grids hierarchy depends on the type of used scheme. We can use, for example, Correction Scheme (CS), where only the residue is transferred; or Full Approximation Scheme (FAS), where the residue and the solution are transferred. In our study we chose FAS (Trottenberg et al. 2000; Wesseling 2004). There are different ways in which different grids can gone through (here called cycles), among them, V-, W- and F-cycle (Franco et al. 2018a, b). We use the V-cycle by its low computational cost (Trottenberg et al. 2000; Wesseling 2004). We define the smoothing numbers in the restriction (ν_1) and prolongation (ν_2) process, respectively to be the pre- and post-smoothing numbers of the solver. In this paper we use the notation $V(\nu_1, \nu_2)$. Furthermore, we use cr = 2 (standard

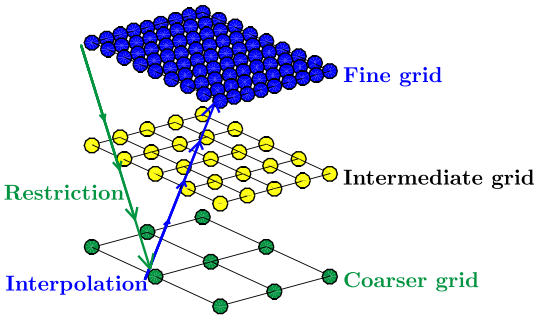

Fig. 1 Representation of the multigrid V-cycle

coarsening), i.e. the coarsening ratio with $H = 2h$ (Trottenberg et al. 2000; Wesseling 2004), where h and H are the distances between the consecutive points of the fine and the coarse grid, respectively.

Figure 1 depicts a V-cycle for the case of $l = 3$ grid coarsening levels. Algorithm 1 is based on the V-cycle for the FAS-scheme considering $l > 1$ grid levels, where I_h^{2h} and I_{2h}^{h} are, respectively, the restriction and prolongation operators. In this case, L_{max} means the maximum number of levels. In both Fig. 1 and Algorithm 1, the standard coarsening is considered.

Algorithm 1: FAS-MG(l) Briggs et al. (2000); Zen et al. (2024).

Input: $\boldsymbol{\psi}_0^h, A_h, \boldsymbol{f}^h$
Output: $\boldsymbol{\psi}^h$
1 **while** *Stopping criterion is not reached* **do**
2 **if** $l = L_{max}$ **then**
3 Solve the system $A_l \boldsymbol{\psi}^l = \boldsymbol{f}^l$ on the coarse grid $\Omega^{2^{l-1}h}$;
4 Compute the correction on the coarse grid $\omega^l = \boldsymbol{\psi}^l - \dot{\boldsymbol{\psi}}^l$;
5 **else**
6 Smooth ν_1 times $A_l \boldsymbol{\psi}^l = \boldsymbol{f}^l$ on the grid $\Omega^{2^{l-1}h}$ with initial guess $\boldsymbol{\psi}_0^l = 0$;
7 Compute and restrict the defect $\dot{\boldsymbol{r}}^{l+1} = I_{2^{l-1}h}^{2^l h}[\boldsymbol{f}^l - A_l \boldsymbol{\psi}^l]$;
8 Restrict the solution $\dot{\boldsymbol{\psi}}^{l+1} = I_{2^{l-1}h}^{2^l h} \boldsymbol{\psi}^l$;
9 Compute the right-hand side $\boldsymbol{f}^{l+1} = \dot{\boldsymbol{r}}^{l+1} + A_{l+1} \dot{\boldsymbol{\psi}}^{l+1}$;
10 Solve at the next level FAS-MG(l+1);
11 Interpolate the correction $\omega^l = I_{2^l h}^{2^{l-1}h} \omega^{l+1}$;
12 Correct the solution $\boldsymbol{\psi}^l \leftarrow \boldsymbol{\psi}^l + \omega^l$;
13 Smooth ν_2 times on $A_l \boldsymbol{\psi}^l = \boldsymbol{f}^l$ on the grid $\Omega^{2^{l-1}h}$ with initial guess $\boldsymbol{\psi}^l$ (updated in line 12);
14 Compute the correction $\omega^l = \boldsymbol{\psi}^l - \dot{\boldsymbol{\psi}}^l$;
15 **end**
16 **end**

Our study presents the standard geometric MG (Wesseling and Oosterlee 2001; Santiago et al. 2015), which is generally advisable in cases where structured grids are used. However, when unstructured grids are used, we can apply the algebraic MG (Marchi et al. 2013a; Stüben 2001; Suero et al. 2012).

In this work, the process of transferring information from the fine grid to the coarser grid (restriction) will be done using the full-weighting operator, defined by Trottenberg et al. (2000), Wesseling (2004)

$$\mathbf{I}_h^{2h}\mathbf{v}_h(x,y) = \frac{1}{16}\begin{bmatrix} 1 & 2 & 1 \\ 2 & 4 & 2 \\ 1 & 2 & 1 \end{bmatrix}_h^{2h}. \tag{25}$$

The process of transferring information from the coarse grid to the finer grid (prolongation) will be done using bilinear interpolation operator, defined by Trottenberg et al. (2000), Wesseling (2004)

$$\mathbf{I}_{2h}^{h}\mathbf{v}_h(x,y) = \frac{1}{2}\begin{bmatrix} 0 & 1 & 0 \\ 1 & 0 & 1 \\ 0 & 1 & 0 \end{bmatrix}_{2h}^{h}. \tag{26}$$

4.2 Effective order of accuracy

It is possible to approximate the asymptotic order of accuracy of each numerical method by the effective and apparent orders (Marchi and da Silva 2002), respectively. The basis for the approximation is the numerical error (difference between analytical and numerical solutions) or by estimating the error of the numerical solution. The equivalent effective order (based on the numerical error) is given by da Silva et al. (2022), Pereira da Silva et al. (2023).

$$p_E = \frac{log\left(\frac{|E(\boldsymbol{\psi}_1(\mathbf{x}_s))|}{|E(\boldsymbol{\psi}_2(\mathbf{x}_s)|}\right)}{log(q)} \rightarrow p_0, \quad \text{if } h \rightarrow 0, \tag{27}$$

where $E(\boldsymbol{\psi}_i) = \boldsymbol{\Psi}_i - \boldsymbol{\psi}_i$ is true numerical error, $\boldsymbol{\Psi}$ the analytical solution, and $\boldsymbol{\psi}_1$, $\boldsymbol{\psi}_2$ the numerical solutions of the variable of interest in coarse (Ω^{h_1}), and fine grid (Ω^{h_2}), respectively. $\mathbf{x}_s$ is the position vector that has coincident coordinates on all meshes chosen to discretize the domain. The constant $q = h_1/h_2$ is the refinement ratio. In addition, h_1 and h_2 represent the spacing of coarse and fine grids, respectively.

For cases where the analytical solution is unknown, it is possible to calculate the equivalent apparent order of accuracy p_U. In this study we will analyze only the effective order of accuracy. See more details of p_U in da Silva et al. (2022), Pereira da Silva et al. (2023).

4.3 Completed Richardson extrapolation

The most common approaches in numerical analysis to reduce the numerical error are grid refinement and the use of higher-order numerical schemes, to which Richardson extrapolation (RE) is an alternative. RE is given by Dahlquist and Björck (2008):

$$\boldsymbol{\psi}_\infty = \boldsymbol{\psi}_{g+1} + \frac{\boldsymbol{\psi}_{g+1} - \boldsymbol{\psi}_g}{q^{p_0} - 1}, \tag{28}$$

where $\boldsymbol{\psi}_\infty$ is the estimated analytical solution, $\boldsymbol{\psi}_{g+1}$ and $\boldsymbol{\psi}_g$ are the numerical solutions in the fine grids h_{g+1} and coarse grids h_g, and $q = h_g/h_{g+1}$ is the refinement ratio. This expression is going to be effective when $\boldsymbol{\psi}_g$ contains only discretization errors. There have been recent modifications of RE to reduce numerical errors (da Silva et al. 2020). Roache and Knupp (1993) devised a method based on Eq. (28) across the full temperature field called CRE using a grid with coincident nodes.

Since not all fine mesh points coincide with the coarse points, we need to use a strategy for applying CRE. We could use a correction as in Roache and Knupp (1993). However, this correction has been proved to limit the extrapolation order in da Silva et al. (2020). Therefore, we use CRE (without repetition) proposed in da Silva et al. (2020). The authors suggest the use of a Newton polynomial for obtaining the equivalent node in the coarse mesh. Another strategy would be the use of a least squares polynomial, which is more generic. The use of 2D least squares polynomials with high order methods also provide good results (Borges et al. 2021).

Since our solution is smooth, we compute CRE with (da Silva et al. 2020)

$$\boldsymbol{\psi}_{g,i}^{\mathrm{CRE}} = \boldsymbol{\psi}_{g,i} + \frac{\boldsymbol{\psi}_{g,i} - \boldsymbol{\psi}_{g-1,i}}{q^{p_0} - 1}, \tag{29}$$

where g is the grid level, and $\boldsymbol{\psi}_{g-1,i}$ is the coarse grid equivalent node obtained with the 2D least squares polynomial.

For the 2D least squares, we find the nearest N_i^2 points to $u_{g-1,i}$ and fit a fifth-degree polynomial to obtain its value. As stated in da Silva et al. (2020), the polynomial degree must be $p_m - 1$, where m is the maximum completed Richardson extrapolation level. In our case, $m = 1$ and p_1 depends on each approximation scheme. For the CDS-2, CCDS-4, and EXP-4, we have 4, 6, and 6, respectively. Therefore, a fifth-degree (sixth-order of accuracy) polynomial works for all schemes. See more details in da Silva et al. (2020), da Silva (2022).

4.4 Iteration error and complexity order

In this study, we use the Euclidean norm vector L_2 and the equivalent norms L_1 and L_∞ (Burden et al. 2016) to perform the iteration error analyses. To do this, we evaluate the generic norm L over the difference between the numerical solution at iteration it and $it - 1$.

In all analyses, we evaluate the dimensionless iteration error (Pereira da Silva et al. 2023), that is, L^{it}/L^0, where L^0 is the error at iteration $it = 0$ with $\boldsymbol{\psi}(\mathbf{x}_i) = 0$. Note that $L^1/L^0 \approx 1$.

Another issue of interest in the simulations of this study is the equation that measures the complexity order over computational operations. The equation chosen to determine this metric is given by Trottenberg et al. (2000); Wesseling (2004):

$$t_{cpu}(N_t) = c(N_t)^{\overline{p}}, \tag{30}$$

where $t_{cpu}(N_t)$ is the CPU time for each discretization level, $N_t = N_x N_y$ is the number of variables, c a constant of proportionality and $\overline{p}$ the complexity order.

CPU time (t_{cpu}), in this work, is concerned about the time intervals spent with the grids generation (the basis and the auxiliary grids), the appliance of the initial guess, the coefficients evaluation and the solution of the system of linear equations represented by Eqs. (15) and (23), until the achievement of the admitted tolerance. In order to evaluate the t_{cpu}, the subroutine CPU_TIME is employed.

4.5 Grouping CRE with FAS-MG

The completed Richardson extrapolation (CRE) method, which is a post-processing, combines numerical solutions on different grids determining higher orders of precision. To minimize discretization errors, this process requires the use of highly refined meshes. As this can generate a high computational cost, the FAS Multigrid method (FAS-MG) is applied to accelerate convergence and obtain numerical solutions in these meshes with an acceptable

cost. Algorithm 2 details the use of CRE, considering $g = 1, \ldots, G$ distinct meshes; together with the FAS-MG, with a certain $l > 1$ grid coarsening levels for each those g meshes. This Algorithm is used on the variable $\boldsymbol{\psi}$. For example, we have $G = 3$ in the case of meshes N = 9×9, 17×17 and 33×33. In the especific case of 33×33 mesh with standard coarsening ratio, we have following levels hierarchy: 33×33, 17×17, 9×9, 5×5 and 3×3, i.e., $l = 5$ grid coarsening levels used in FAS-MG. In this work, the number of levels adopted in the multigrid method will always be the maximum number of levels (L_{max}). Note that L_{max} depends on g.

Algorithm 2: FAS-MG-CRE.

Input: G, $\boldsymbol{\psi}_0^h$, A_h, $\boldsymbol{f}^h$
Output: $\boldsymbol{\psi}_{g,i}$
Step one: FAS-MG;
begin
  For $g = 1, \ldots, G$;
  $L_{max} = l(g)$;
  $l = 1$;
  Call FAS-MG(l) to calculate $\boldsymbol{\psi}_g$;
  $\boldsymbol{\psi}_{g,i} \leftarrow \boldsymbol{\psi}_g$;
  $g \leftarrow g + 1$;
Step two: CRE;
begin
  For $g = 1, \ldots, G$;
  Calculate $\boldsymbol{\psi}_{g,i}^{\text{CRE}} = \boldsymbol{\psi}_{g,i} + \frac{\boldsymbol{\psi}_{g,i} - \boldsymbol{\psi}_{g-1,i}}{q^{p_0} - 1}$

Remark 2 In the same way that Algorithm 2 was built with FAS-MG, it can also be used with CS-MG.

5 Numerical results

To assure that the numerical solution admit only discretization errors, the absolute value of L^{it}/L^0 was calculated until it achieves its machine round-off error (Pereira da Silva et al. 2023), i.e., *tol=1.0E-32*, for the nodes $N_x = N_y = 9, 17, 33, \ldots, 2049, 4097$ and grids $N = 9 \times 9, 17 \times 17, 33 \times 33, \ldots, 2049 \times 2049, 4097 \times 4097$. The variable of interest is the temperature at center point $\mathbf{x}_s(1/2, 1/2)$. The numerical solutions for problems are obtained using computational programs written by the authors in Fortran 95 and using the Microsoft® Visual Studio® 2008 compiler v.9.0.21022.8 RTM with quadruple precision and are run on a computer with a 3.40 GHz Intel® Core™i7-6700 processor with 16GB of RAM hosting 64-bit Windows® 10. In all three numerical methods used in this study (CDS-2, CCDS-4, and EXP-4), we associated the same computational meshes. This means that we discretize the domain using identical meshes ranging from 9×9 to 4097×4097 nodes, always with constant refinement ratio $q = 2$, i.e., $h_2 = h_1/2$. As such, the mesh element h_2 is associated with the 17×17 discretization and h_1 associated with the discretization with 9×9 nodes, respectively.

We calculate the approximations for systems $A\boldsymbol{\psi} = \mathbf{f}$, where $A_{N \times N}$ is the matrix of coefficients, $\boldsymbol{\psi}_{N \times 1}$ is the numerical solution vector that represents the temperature and $\mathbf{f}_{N \times 1} = f(x_i, y_j) = f_{i,j}$ is the source term in lexicographic order.

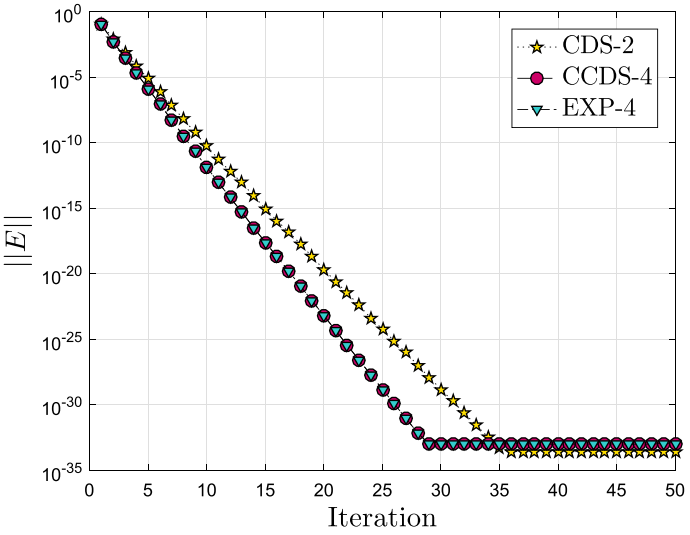

Fig. 2 Iteration error using Gauss-Seidel smoother in 4097 × 4097 grid for three methods

Verification of the numerical solutions is a methodology that allows you to evaluate the coherence of the solutions determined (da Silva 2022; da Silva et al. 2022; Pereira da Silva et al. 2023). This methodology is divided into two steps. The first one is called qualitative verification of numerical solutions (Pereira da Silva et al. 2023). It consists in evaluating numerical errors, orders of accuracy obtained *a priori* and *a posteriori*, as well as analyses on the graphs of decreasing norm of the discretization error *versus* decreasing h. The second one is the quantitative verification of numerical solutions (Pereira da Silva et al. 2023). In this step, we have the opportunity to evaluate the established metrics to inform whether the solutions converge within the expected time. In this work we will assume the following analytical solution $\boldsymbol{\Psi}(x, y) = cos(x)cos(y)$ with $f(x, y) = -cos(x + y) + cos(x - y)$.

5.1 Qualitative verification

Firstly, we analyze the reduction in the magnitude of the iteration error *versus* the number of iterations for CDS-2 method. We set a large enough number of iterations to see the error fluctuate on the order of magnitude of the round-off error by adopting the quadruple precision of the Fortran language to perform the calculations. With this strategy, it can be stated that the iteration error is negligible because its effects cannot contaminate the solutions. See these details in Fig. 2. In our study, the iteration error is very important, because we need to make sure that such an error is oscillating on the order of magnitude of the round-off error, or else the completed Richardson extrapolation will not determine the results we want to obtain.

In Fig. 3 we show the decrease in the norm of the true error of the variable $\boldsymbol{\psi}(\mathbf{x}_s)$ *versus* decreasing the mesh element size for all three cases. Note that reference curves are inserted in this figure. We did this for L_1, L_2 and L_∞, at the $m = 0$ and $m = 1$ level. The $m = 0$ level has no completed Richardson extrapolation, while at $m = 1$, the temperature field has been completely extrapolated only once. Since the three norms are equivalent, exactly the results that are shown in the figure are expected, i.e. the magnitude of the norms of the error are approximately the same for both $m = 0$ and $m = 1$. Moreover, for the most refined mesh, we

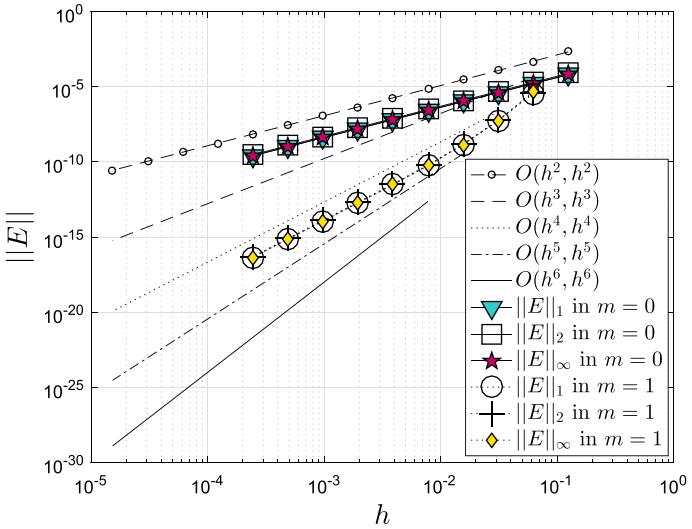

Fig. 3 Norm of the discretization error *versus* h using CDS-2

were able to reduce more than six-orders of magnitude of these norms of the discretization error. Notice that with each extrapolation, we lose the solution associated with the coarsest mesh of this level. For example, in level $m = 1$, the solution associated with the mesh 9×9 is lost. This is part of all types of extrapolation, whether nodal or complete.

The equivalent effective orders of accuracy shown in Fig. 4 are obtained *a posteriori* and can only be calculated in cases where the analytical solution is known. In order not to make the term exhaustive, we decided to call these orders just effective orders, and therefore we will use this term from here on. See more details in da Silva et al. (2021), Marchi (2001), da Silva et al. (2022), da Silva (2022). The order of accuracy of the CDS-2 method is $p_0 = 2$ as we already know. We did the p_E calculations using three norm rules to confirm the equivalence of the rules in this case. When we applied the CRE method, the order $p_0^* = 2$ jumped to $p_1^* = 4$, as the truncation error terms that have odd powers cancel each other out, leaving only the even powers that denote the set of *a posteriori* true orders $p_m^* = \{p_0^*, p_1^*, p_2^*, \ldots\} = \{2, 4, 6, \ldots\}$ that can be deduced *a priori*. Thus, when performing the completed Richardson extrapolation, we expect exactly this behavior, i.e., the increase of two orders of accuracy. The asymptotic behavior of the fourth-order of accuracy curves is expected and does not represent numerical error. This means that p_1 (*a priori*) and p_1^* (*a posteriori*) are equal in the limit, in other words,

$$\lim_{h \to 0} \varepsilon_\tau(\boldsymbol{\Psi}) = \sum_{m=0}^{\infty} \lim_{h \to 0} c_m \, h^{p_m} = 0, \tag{31}$$

where c_m is an arbitrary constant that does not depend on h and p_m is the *a priori* order of accuracy of the method. In the case of infinitely many terms of the truncation error, we have the following expression:

$$\lim_{h \to 0} \varepsilon_\tau(\boldsymbol{\Psi}) = \lim_{h \to 0} \left(c_0 \, h^{p_0} + c_1 \, h^{p_1} + c_2 \, h^{p_2} + \ldots + c_m \, h^{p_m} \right) = 0. \tag{32}$$

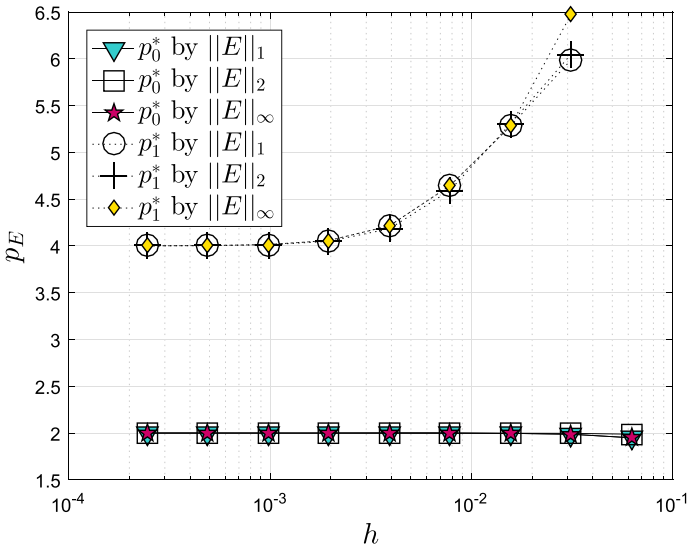

Fig. 4 Equivalent effective order of accuracy using CDS-2

For example, we will revisit Eq. (5) (which is a sum of errors of the Eqs. (2) and (3) for $h = k$) that represents the truncation error and which rewritten as a function of Eq. (32), results in

$$\varepsilon_\tau(\boldsymbol{\Psi}) = -\frac{1}{12}\left(\frac{\partial^4 \boldsymbol{\Psi}}{\partial x^4} + \frac{\partial^4 \boldsymbol{\Psi}}{\partial y^4}\right) h^{p_0=2} - \frac{1}{360}\left(\frac{\partial^6 \boldsymbol{\Psi}}{\partial x^6} + \frac{\partial^6 \boldsymbol{\Psi}}{\partial y^6}\right) h^{p_1=4} + c_2\, h^{p_2=6} + \cdots + c_m\, h^{p_m}, \tag{33}$$

with

$$\lim_{h\to 0}\left(c_0\, h^{p_0} + c_1\, h^{p_1} + c_2\, h^{p_2} + \cdots + c_{m-1}\, h^{p_{m-1}} + c_m\, h^{p_m}\right) = 0, \tag{34}$$

where $c_0 = -1/12(\partial^4 \boldsymbol{\Psi}/\partial x^4 + \partial^4 \boldsymbol{\Psi}/\partial y^4)$, and $c_1 = -1/360(\partial^6 \boldsymbol{\Psi}/\partial x^6 + \partial^6 \boldsymbol{\Psi}/\partial y^6)$, respectively.

Equation (33) shows what equivalent order of accuracy we should find when applying CRE to get the solutions at the $m = 1$ level to CDS-2. This result is confirmed in Fig. 4.

Now we will reproduce the same analyses as for the CDS-2 method for CCDS-4. The profile of results was consistent with that expected for the fourth-order of accuracy method, see Fig. 5. Note that reference curves are inserted in this figure. That is, the straight lines corresponding to the norms of the discretization error at $m = 1$ are steeper slope and the difference of the orders of magnitude of these errors in the more refined meshes become smaller. Using CDS-2 the difference was about 6 orders of magnitude, while for CCDS-4 around 2 orders. This occurs because the term $c_0\, h^{p_0=2}$ has more influence than $c_0\, h^{p_0=4}$. This behavior is correct and expected.

If we were to rewrite the Eq. (33) for the CCDS-4 method, it would certainly not be difficult to see that by applying CRE the order of accuracy would jump from $p_0^* = 4$ to $p_1^* = 6$. These results are confirmed in Fig. 6 when we calculate the effective orders. Note that for the most refined mesh at $m = 1$ the orders exhibit degeneration for some norms. We call degeneration the mathematical phenomenon that makes an order present random results due to the influence of round-off error that is contaminating the numerical operations

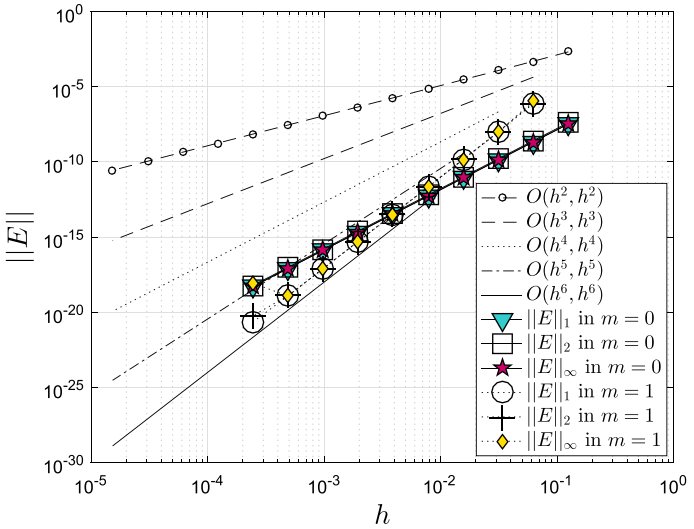

Fig. 5 Norm of the discretization error *versus* h using CCDS-4

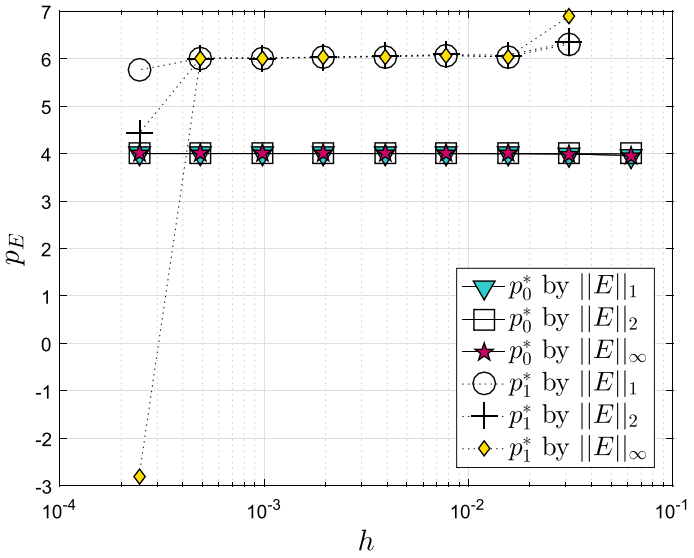

Fig. 6 Equivalent effective order of accuracy using CCDS-4

or solutions (da Silva et al. 2022). If we were using double precision, this degeneration would have happened on coarser meshes.

To finalize the qualitative verification of the numerical solutions of our mathematical model using the three numerical methods, we will see at the decrease in discretization error *versus* decrease in h to EXP-4. See in Fig. 7 that the results are equivalent to those shown in Fig. 5 (note that reference curves are inserted in this figure). This means that both methods behave very similarly, with proven consistency and accuracy.

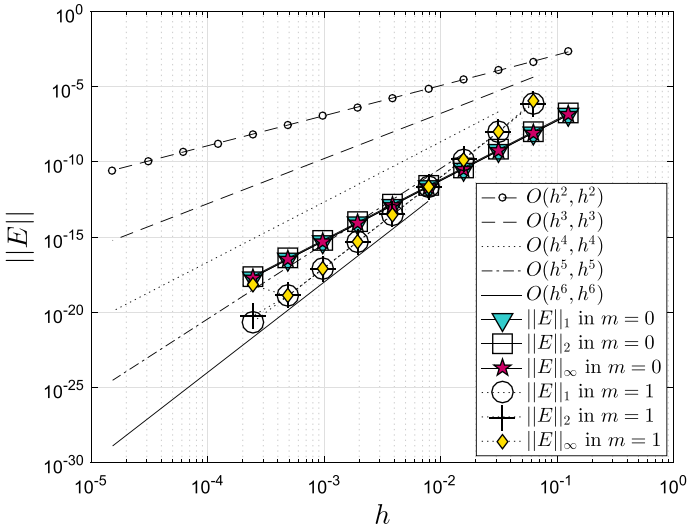

Fig. 7 Norm of the discretization error *versus* h using EXP-4

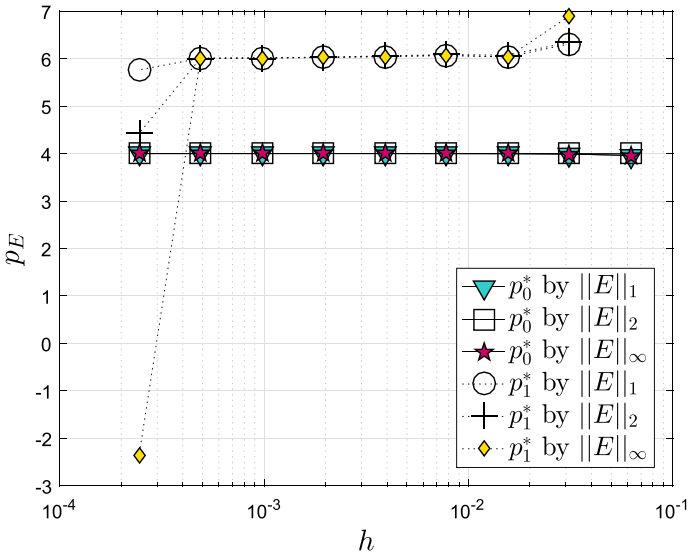

Fig. 8 Equivalent effective order of accuracy using EXP-4

In Fig. 8, again we find a case of equivalence of results. Notice that the curves of the effective orders p_E have the same behavior as the ones shown in Fig. 6. Visually identical, however, there is a small numerical difference that is imperceptible when comparing the two figures.

To confirm the results presented in this study, Table 1 shows the reduction in error using, for example, norm L_2 with and without application of the CRE, thus corroborating the error orders given by Figs. 4, 6, and 8.

Table 1 Discretization error using $||E||_2$ without ($m = 0$) and with CRE ($m = 1$)

h	CDS-2		CCDS-4		EXP-4	
	$m = 0$	$m = 1$	$m = 0$	$m = 1$	$m = 0$	$m = 1$
1.25E-01	*7.82E-05*	–	*4.11E-08*	–	*1.64E-07*	–
6.25E-02	*1.97E-05*	*4.03E-06*	*2.57E-09*	*8.47E-07*	*1.02E-08*	*8.47E-07*
3.12E-02	*4.94E-06*	*6.09E-08*	*1.60E-10*	*1.03E-08*	*6.43E-10*	*1.03E-08*
1.56E-02	*1.23E-06*	*1.53E-09*	*1.00E-11*	*1.54E-10*	*4.02E-11*	*1.54E-10*
7.81E-03	*3.08E-07*	*6.37E-11*	*6.28E-13*	*2.27E-12*	*2.51E-12*	*2.27E-12*
3.90E-03	*7.72E-08*	*3.50E-12*	*3.92E-14*	*3.40E-14*	*1.57E-13*	*3.40E-14*
1.95E-03	*1.93E-08*	*2.12E-13*	*2.45E-15*	*5.20E-16*	*9.82E-15*	*5.20E-16*

Table 2 CPU time (s) to determine numerical solutions of of p_0^*-th order by MG and (p_{0+1}^*)-th order of accuracy using CRE in the 4097×4097 mesh

Method	Solution of p_0^*-th order by MG	Solution of (p_{0+1}^*)-th order by CRE
CDS-2	$3.13E+03$	$2.63E+03$
CCDS-4	$4.31E+03$	$3.22E+03$
EXP-4	$4.59E+03$	$3.26E+03$

5.2 Quantitative verification

A first metric chosen to perform the quantitative verification of our numerical solutions is the CPU time. In Table 2 we present the CPU time (in seconds) to obtain the numerical solution in the 4097×4097 mesh using MG considering *tol=1.0E-32* (round-off error) and the post-processing CRE time using maximum number of meshes to extrapolations, i.e., 10 meshes. In this section we are only interested in the discretization error to be able to apply the CRE, therefore, the other sources of numerical errors must be neglected. To do this, it is indispensable to achieve round-off error. Therefore, specifically in this section, it does not make sense to calculate CPU time, as it is not representative when such error level is reached. We can see in Table 2 that the second and third columns have the same order of magnitude taking into account that the numerical solutions (second column) were obtained with geometric multigrid method. Otherwise, the CRE CPU time would be considerably shorter.

The second metric chosen to perform the quantitative verification of our numerical solutions is the so-called complexity order (Trottenberg et al. 2000; Wesseling 2004) when we make use of the Eq. (30). This metric tells us that MG should be able to determine numerical solutions and the value of $\overline{p}$ should be close to unity. Singlegrid methods (standard method with only one grid) have quadratic complexity order. This verification is classic and ensures that the MG is performing with proven efficiency its role as an accelerator of convergence of numerical solutions.

For this we use $V(2, 1)$, i.e., V-cycle with 2 and 1 pre- and post-smoothing, respectively. And all simulations we set the maximum number of iterations equal to 50. This number was chosen because it was large enough to the iteration error reaches the order of magnitude of the round-off error (oscillation around *1.0E-32*).

Table 3 Complexity order for all methods using *tol=1.0E-32*

Method	c	$\overline{p}$
CDS-2	$1.4730E-04$	1.0140
CCDS-4	$1.8480E-04$	1.0240
EXP-4	$2.3320E-04$	1.0060

Note that in Table 3 we show that the EXP-4 method determines complexity order closer to unity than the CCDS-4 method. This result confirms the advantage of EXP-4, as already stated in da Silva et al. (2021).

To finish our analyses, we leave the specific evidence of the verification of numerical solutions. In the first part of the verification (qualitative verification) we confirm the orders of accuracy obtained *a posteriori* with those deduced *a priori*. In the second part (quantitative verification), we confirm by quantitative verification, the efficiency of the geometric MG by means of the metric complexity order. We are confident that such methodology ennobles the results of numerical simulations that can be extended to any mathematical model. When the analytical solution is unknown, simply replace the effective order (p_E) with the apparent order (p_U). The p_U should be able to reproduce the *a priori* deduced orders of accuracy, just as the p_E makes such a result possible.

We understand that the results we show in our study, determine benchmark solutions for the high order of accuracy methods after applying completed Richardson extrapolation.

6 Conclusions

This study proposed a grouping of methods for determining numerical solutions to the Poisson heat diffusion equation with high accuracy. We compared the results obtained with classical second-order finite difference method (CDS-2) with fourth-order compact (CCDS-4) and the exponential methods (EXP-4). We accelerated the convergence of the numerical solutions using multigrid method. After ensuring that the verification of numerical solutions performed its function with excellence, we applied the completed Richardson extrapolation (CRE) across the full temperature field. In our study we confirmed the efficiency verification of the numerical solution methodology by demonstrating the consistency of the numerical results with the analytical ones. This proves that our proposed methodology is robust enough to allow all steps of the numerical simulation to be very well evaluated. We were able to confirm that the EXP-4 method is more advantageous than CCDS-4. Moreover, we are dealing with a method that is little known in the literature. With this, the numerical solutions for the Poisson equation was obtained using a computational mesh with *16,785,409* nodes. Computational effort was low and we jumped from fourth- to sixth-order of accuracy simply by employing CRE as post-processing method. We believe that EXP-4, together with CRE, can motivate new studies in the scientific community and thus present results for increasingly complex mathematical models.

Acknowledgements Federal University of Parana and Numerical Experimentation Laboratory by financial and physical support.

Funding The authors received no specific funding for this study.

Data availability Not applicable.

Declarations

Conflict of interest The authors declare that they have no conflict of interest to report regarding the present study.

References

Borges RBR, da Silva NDP, Gomes FAA, Shu C-W, Tan S (2021) A sequel of inverse Lax-Wendroff high order wall boundary treatment for conservation laws. Archives of Computational Methods in Engineering. https://doi.org/10.1007/s11831-020-09454-w

Briggs WL, Henson VE, McCormick SF (2000) A Multigrid Tutorial, pp. 95–111

Burden RL, Faires JD, Burden AM (2016) Numerical Analysis, 10th edn

Chemeda HM, Negassa AD, Merga FE (2022) Compact finite difference scheme combined with Richardson extrapolation for Fisher's equation. Mathematical Problems in Engineering 2022

Chemeda HM, Merga FE (2021) Fourth-order compact finite difference method combined with Richardson extrapolation for one-dimensional heat equation. OMO Int J Sci 4(1):76–90

Cheney EW, Kincaid DR (2012) Numerical Mathematics and Computing

da Silva LP (2022) Verification of numerical solutions in diffusive problems solved with the smoothed particle hydrodynamics method (in portuguese). PhD thesis, Federal University of Paraná, Curitiba, Brazil. https://acervodigital.ufpr.br/handle/1884/74829

da Silva NPD (2022) Repeated completed Richardson extrapolation for flows with compressible fluid (in portuguese). PhD thesis, Federal University of Paraná, Curitiba, Brazil. https://acervodigital.ufpr.br/handle/1884/59720

da Silva NDP, Marchi CH, Araki LK, Borges RBR, Bertoldo G, Shu C-W (2020) Completed repeated Richardson extrapolation for compressible fluid flows. Appl Math Model 77:724–737

da Silva LP, Rutyna BB, Righi ARS, Pinto MAV (2021) High order of accuracy for poisson equation obtained by grouping of repeated Richardson extrapolation with fourth order schemes. CMES-Computer Modeling in Engineering & Sciences 128(2):699–715

da Silva LP, Marchi CH, Meneguette M, Foltran AC (2022) Robust RRE technique for increasing the order of accuracy of SPH numerical solutions. Math Comput Simul 199:231–252. https://doi.org/10.1016/j.matcom.2022.03.016

da Silva L, Marchi C, Meneguette M, Suero R (2024) Fast convergence of SPH numerical solutions using robust algebraic multilevel. Journal of Computational Science, 102369

Dahlquist G, Björck Å (2008) Numerical Methods in Scientific Computing, Volume I

Dai R, Lin P, Zhang J (2017) An efficient sixth-order solution for anisotropic poisson equation with completed Richardson extrapolation and multiscale multigrid method. Computers & Mathematics with Applications 73(8):1865–1877

Franco SR, Gaspar FJ, Pinto MAV, Rodrigo C (2018) Multigrid method based on a space-time approach with standard coarsening for parabolic problems. Appl Math Comput 317:25–34

Franco SR, Rodrigo C, Gaspar FJ, Pinto MAV (2018) A multigrid waveform relaxation method for solving the poroelasticity equations. Comput Appl Math 37(4):4805–4820

Gordin V, Shadrin D (2023) Compact approximation of a two-dimensional boundary value problem for elliptic equations of the second order with a discontinuous coefficient. Math Models Comput Simul 15(5):920–943

Gupta MM, Kouatchou J, Zhang J (1997) Comparison of second and fourth order discretizations for multigrid Poisson solvers. J Comput Phys 132(2):226–232. https://doi.org/10.1006/jcph.1996.5466

Hu H, Li M, Pan K, Wu P (2022) An extrapolation accelerated multiscale Newton-MG method for fourth-order compact discretizations of semilinear Poisson equations. Computers & Mathematics with Applications 113:189–197

Hu S, Pan K, Wu X, Ge Y, Li Z (2023) An efficient extrapolation multigrid method based on a hoc scheme on nonuniform rectilinear grids for solving 3d anisotropic convection-diffusion problems. Comput Methods Appl Mech Eng 403:115724

Koroche KA, Chemeda HM (2021) Six-order compact finite difference method for solving KDV-Burger equation in the application of wave propagations. Iranian Journal of Numerical Analysis and Optimization

Le Veque RJ (2007) Finite Difference Methods for Ordinary and Partial Differential Equations: Steady-state and Time-dependent Problems

Li J, Chen Y (2008) Computational Partial Differential Equations Using MATLAB

Malacarne MF, Pinto MA, Franco SR (2022) Performance of the multigrid method with time-stepping to solve 1d and 2d wave equations. Int J Comput Methods Eng Sci Mech 23(1):45–56
Marchi CH (2001) Verification of unidimensional numerical solutions in fluid dynamics (in portuguese). PhD thesis, Federal University of Santa Catarina, Florianópolis, Brazil. URL: http://ftp.demec.ufpr.br/CFD/monografias/2001_Carlos_Marchi_doutorado.pdf
Marchi CH, da Silva AFC (2002) Unidimensional numerical solution error estimation for convergent apparent order. Numerical Heat Transfer: Part B: Fundamentals 42(2):167–188
Marchi CH, Araki LK, Alves AC, Suero R, Gonçalves SFT, Pinto MAV (2013) Repeated Richardson Extrapolation applied to the two-dimensional Laplace equation using triangular and square grids. Appl Math Model 37:4661–4675
Marchi CH, Novak LA, Santiago CD, Vargas APS (2013) Highly accurate numerical solutions with repeated Richardson Extrapolation for 2D Laplace equation. Appl Math Model 37:7386–7397
Marchi CH, Martins MA, Novak LA, Araki LK, Pinto MAV, Gonçalves SFT, Moro DF, Freitas IS (2016) Polynomial interpolation with repeated Richardson extrapolation to reduce discretization error in CFD. Appl Math Model 40(21–22):8872–8885
Oliveira ML, Pinto MAV, Gonçalves SFT, Rutz GV (2018) On the robustness of the xy-zebra-Gauss-Seidel smoother on an anisotropic diffusion problem. Computer Modeling in Engineering & Sciences 117(2):251–270
Pandey PK (2013) A higher accuracy exponential finite difference method for the numerical solution of second order elliptic partial differential equations. Journal of Mathematical and Computational Science 3(5):1325–1334. visited on 06-15-2021
Pandey PK (2016) Solving two point boundary value problems for ordinary differential equations using exponential finite difference method. Boletim da Sociedade Paranaense de Matemática 34(1):45–52. https://doi.org/10.5269/bspm.v34i1.22424
Pandey PK, Pandey BD (2016) Variable mesh size exponential finite difference method for the numerical solutions of two point boundary value problems. Boletim da Sociedade Paranaense de Matemática 34(2):9–27. https://doi.org/10.5269/bspm.v34i2.24599
Pereira da Silva L, Meneguette Junior M, Marchi CH (2023) Numerical Modeling of Heat Diffusion, pp. 7–49. Springer, Cham. https://doi.org/10.1007/978-3-031-28946-0_2
Pereira da Silva L, Meneguette Junior M, Marchi CH (2023) Numerical Error Analysis and Heat Diffusion Models, pp. 51–75. Springer, Cham. https://doi.org/10.1007/978-3-031-28946-0_3
Pereira da Silva L, Meneguette Junior M, Marchi CH (2023) SPH Applied to Computational Heat Transfer Problems, pp. 77–115. Springer, Cham.https://doi.org/10.1007/978-3-031-28946-0_4
Pinto M, Rodrigo C, Gaspar F, Oosterlee C (2016) On the robustness of ilu smoothers on triangular grids. Appl Numer Math 106:37–52
Roache PJ, Knupp PM (1993) Completed Richardson Extrapolation. Commun Numer Methods Eng 9(5):365–374
Santiago CD, Marchi CH, Souza LF (2015) Performance of geometric multigrid method for coupled two-dimensional systems in CFD. Appl Math Model 39:2602–2616. https://doi.org/10.1016/j.apm.2014.10.067
Santiago CD, Ströher GR, Pinto MA, Franco SR (2023) A multigrid waveform relaxation method for solving the pennes bioheat equation. Numerical Heat Transfer, Part A: Applications 83(9):976–990
Stüben K (2001) A review of algebraic multigrid. Journal of Computation and applied Mathematics 128:281–309
Suero R, Pinto MAV, Marchi CH, Araki LK, Alves AC (2012) Analysis of algebraic multigrid parameters for two-dimensional steady-state heat diffusion equations. Appl Math Model 36(7):2996–3006
Trottenberg U, Oosterlee CW, Schuller A (2000) Multigrid
Wang Y, Zhang J (2009) Sixth order compact scheme combined with multigrid method and extrapolation technique for 2D Poisson equation. J Comput Phys 228:137–146. https://doi.org/10.1016/j.jcp.2008.09.002
Wesseling P (2004) An Introduction to Multigrid Methods
Wesseling P, Oosterlee CW (2001) Geometric multigrid with applications to computacional fluid dynamics. Journal od Computation and applied Mathematics 128:311–334
Zen PD, Pinto MAV, Franco SR (2024) A multigrid waveform relaxation method for solving the nonlinear silicon problem with relaxing boundary conditions. Numerical Heat Transfer, Part B: Fundamentals, 1–16